CCAT Sunyaev-Zeldovich Effect Science and Telescope Requirements *

Sunil Golwala

June 22, 2005

1   Science Goals

Sunyaev-Zeldovich effect observations with CCAT will naturally focus on four science goals:

- Detailed thermal Sunyaev-Zeldovich (tSZ) effect mapping of clusters detected by large-area blind tSZ surveys such as APEX-SZ, ACT, SPT, and Planck. CCAT follow-up will provide detailed SZ profiles that will greatly aid in interpreting these surveys.

- Blind tSZ surveys reaching a lower mass limit than the aforementioned large-area surveys.

- Measurement of the tSZ anisotropy power spectrum at very high angular multipole number, $\ell \sim 2000 - 20000$.

- Low-resolution tSZ spectroscopic follow-up of clusters to aid in measuring relativistic effects and to possibly provide SZ-based gas temperatures.

Other science goals have been considered (primary CMB anisotropy, kSZ searches in known clusters, kSZ anisotropy, SZ polarization) but are either better accomplished by other instruments or simply beyond the reach of CCAT.

2   Motivation and Background

The Sunyaev-Zeldovich effects consist of scattering of cosmic microwave background (CMB) photons by the hot electrons in the intracluster medium (ICM) of galaxy clusters. The thermal SZ (tSZ) effect is a spectral distortion of the CMB due to the shift in photon energy by Compton scattering. The kinetic SZ (kSZ) effect is a Doppler shift of the CMB due to scattering by a moving cluster. Frequency spectra of the tSZ and kSZ effects, and of the CMB, are shown in Figure 1.

The tSZ effect has been detected in tens of clusters; John Carlstrom's group at University of Chicago dominates the count, having used the BIMA and OVRO interferometers to image about 60 clusters at 30 GHz. The SuZIE experiment has the largest millimeter-wave sample, with a total of 11 clusters with measurements at 150, 220, and 275 GHz. No cluster has been found "blindly" in the tSZ yet. The kSZ effect has not been detected. A significant deficiency of the existing data is their relatively poor angular resolution (about 1 arcmin) and their lack of ability to probe extended structure (because the sample is dominated by interferometric measurements).

There is a very compelling case to be made for the study of galaxy clusters using tSZ. The tSZ effect essentially measures the line-of-sight integral of the gas pressure in a cluster. This is

---

*A companion technical note, with details on calculational methods, is provided in S. Golwala, *Basic Features of the Sunyaev-Zeldovich Effects Relevant to the CCAT*, available from the same web site as this note. The companion technical note is referenced elsewhere in this note.
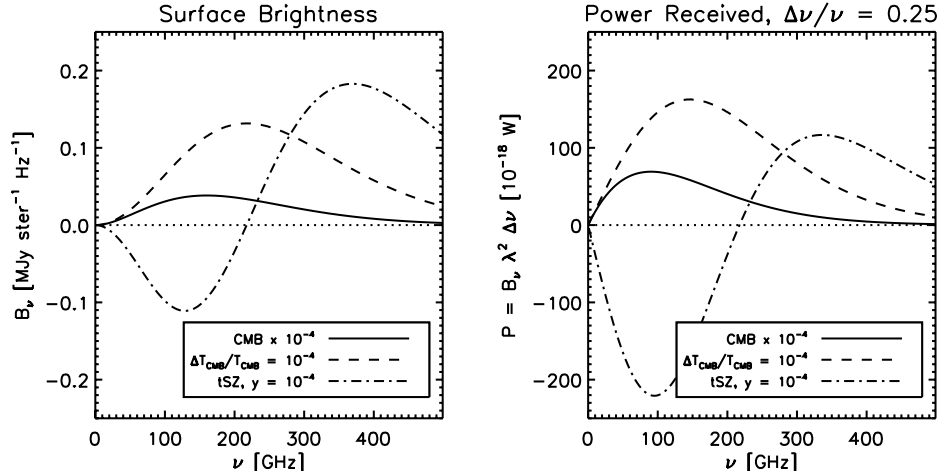
Figure 1: CMB and SZ frequency spectra. Solid curve: CMB. Dashed curve: CMB temperature anistropy at $\Delta T_{\mathrm{CMB}}/T_{\mathrm{CMB}} = 10^{-4}$ (comparable to primary anisotropy on 1 degree angular scales). Dash-dot curve: thermal SZ (tSZ) effect for $y = 10^{-4}$ ($\tau = 0.005$ and $T_e \sim 10$ keV $\approx 0.02\, m_e\, c^2$), typical of a massive, nearby cluster. The dashed curve also holds for kinetic SZ (kSZ) with $(v/c)\,\tau = 10^{-4}$ (a massive cluster with $\tau = 0.005$ and $v = 600$ km/s, larger than expected by a factor of a few). Right: power incident on a receiver assuming 25% fractional bandwidth and single-optical-mode design.

an observable that is central to any understanding of gas dynamics in the intracluster medium. Historically, free-free X-ray emission is our primary probe of intracluster gas. X-ray emission is a complicated observable: it measures the product of the square of the electron density, n_e^2, and the nontrivial electron-temperature dependent emissivity function, $\Lambda(E_X, T_e)$. While Chandra and XMM have taught us a great deal, they have also more than adequately proven how complicated the ICM is, with cold fronts, bubbles from AGN, evidence of mergers, etc. tSZ would provide us with another ICM observable, one that is more simply related to a physical quantity (the pressure) than X-ray emission. tSZ profiles of clusters would allow more detailed study of the thermodynamic state of the gas, including the level of entropy injection by star formation or other heating processes, the importance of radiative cooling, and cluster merger histories. tSZ may also give us more information about the shape of the gravitational potential well – the dark matter – and the gas profile, as tSZ will naturally extend out to larger radius than X-ray emission.

Regular observation of the kSZ effect, while extremely challenging, would provide a new and unique observable for cosmology: a probe of the peculiar velocity field at high redshift (z up to 2 or 3). It may also be possible to study internal bulk motions in galaxy clusters using the kSZ effect.

An exciting prospect for SZ work in the coming years is the advent of large-area "blind" surveys in the tSZ. The tSZ provides a largely redshift-independent method for detecting galaxy clusters; a flux-limited tSZ survey is, to a factor of 2, a mass-limited survey. Thus, measurement of cluster abundance as a function of redshift via the tSZ would be free of the extremely redshift-dependent selection function one finds for optical or X-ray surveys for clusters. Such a cluster abundance measurement would constrain cosmological parameters, in particular Ω_m, Ω_Λ, and the equation of state parameter w. A number of such surveys will be undertaken in the coming years by the Atacama Pathfinder Experiment-SZ (APEX-SZ – MPIfR and Berkeley), the Atacama Cosmology Telescope (ACT – Princeton, Penn, Goddard), the South Pole Telescope (SPT – Chicago, Case Western, and Berkeley), and the Planck satellite.

Interpretation of these surveys will require careful characterization of the tSZ mass determina-

tion. The surveys intentionally leave the emission spatially unresolved in order to maximize survey efficiency. Thus, they obtain little information about the tSZ emission aside from its total flux. Follow-up imaging using CCAT would provide angular resolution 3-4 times better than the surveys will have. This detailed tSZ information will be critical for understanding how cluster astrophysics affect the tSZ mass determination. Such information will be essential for cosmological intepretation of survey yields.

3   Sunyaev-Zeldovich Observables

There is a large literature on calculating the expected dark-matter and gas profiles of galaxy clusters, the resulting tSZ and kSZ profiles, and the abundances of clusters. We have reviewed this literature in a technical note and calculated simple approximate formulae for basic quantities of interest. Based on these, we present numerical estimates of various SZ observables – cluster abundances, cluster sizes, and signal levels.

3.1   Assumptions

The fiducial cluster we would like to detect is one at the mass limit of the wide-area tSZ surveys such as APEX-SZ, ACT, and SPT, with $M \approx 3.5 \times 10^{14}$ M$_\odot$. Other fiducial targets would be clusters with masses of 10^{14} M$_\odot$, 10^{15} M$_\odot$, and 3.5×10^{15} M$_\odot$. The Planck all-sky survey is expected to detect clusters down to a mass limit of 8×10^{14} M$_\odot$.

For reference, we will assume a Gaussian illumination of a 25-m diameter primary with a conservative -10 dB edge taper. The illumination pattern has $\sigma = 5.8$ m and FWHM = 13.7 m. This results in the beam sizes given in Table 1.

frequency	beam FWHM
275 GHz	0.24 arcmin = 14 arcsec
220 GHz	0.30 arcmin = 18 arcsec
150 GHz	0.44 arcmin = 26 arcsec
100 GHz	0.66 arcmin = 40 arcsec

Table 1: Assumed beam sizes.

As will be discussed below in regard to frequency coverage, Figure 1 indicates that 100–150 GHz is the best frequency range in which to detect the SZ effect, assuming one wants to be in the millimeter-wave regime where tSZ is spectrally separable from kSZ and CMB. Since the SZA will observe at 100 GHz, we focus our discussion on observations at 150 GHz. Further discussion of complementarity between CCAT and SZA is given later.

3.2   Basic Facts about the Sunyaev-Zeldovich Effect

Some basic facts about the SZ effects for later reference:

- Relation between cluster Comptonization parameter y and surface brightness and CMB temperature fluctuations:

$$\frac{\Delta B_\nu}{B_\nu} = h(x)\,\frac{\Delta T_{\mathrm{CMB}}}{T_{\mathrm{CMB}}} = h(x)\,f(x)\,y \qquad y = \int n_e\,\frac{k\,T_e}{m_e\,c^2}\,\sigma_T\,dl \qquad (1)$$

  with

$$B_\nu(x) = 2\,k\,T_{\mathrm{CMB}}\left(\frac{\nu}{c}\right)^2 \frac{x}{e^x - 1} \qquad h(x) = \frac{x\,e^x}{e^x - 1} \qquad f(x) = x\,\frac{e^x + 1}{e^x - 1} - 4 \qquad (2)$$

3

where $x = h\nu/kT_{\mathrm{CMB}}$ is set by the observing frequency and y is the Comptonization parameter of the scattering medium. k is Boltzmann's constant, m_e, n_e, and T_e are the electron mass, density, and temperature, σ_T is the Thomson scattering cross section, and the integral is along the line of sight.

- Relation between cluster optical depth to Thomson scattering, peculiar velocity, and kSZ surface brightness and CMB temperature fluctuations:

$$\frac{\Delta B_\nu}{B_\nu} = h(x)\frac{\Delta T_{\mathrm{CMB}}}{T_{\mathrm{CMB}}} = -h(x)\frac{v}{c}\tau \qquad \tau = \int n_e\,\sigma_T\,dl \qquad (3)$$

where v is the peculiar velocity of the scattering medium, c is the speed of light, and τ is the optical depth for Thomson scattering in the ionized medium. Note that the kinetic effect is "thermal" in the sense that the thermodynamic temperature fluctuation is independent of frequency; hence, the kinetic effect is spectrally indistinguishable from primary CMB fluctuations.

3.3 Numerical Estimates of Abundances, Angular Scales, and Signal Levels

In Table 2, we list some numerical estimates of cluster abundances, angular scales, and signal levels. These estimates are a mix of simple analytic calculations (NFW dark matter profile + β-model gas profile) and simulations (used primarily for normalization purposes). Details are again given in a companion technical note. All cluster parameters are dependent on the redshift of cluster formation (z_f) and of observation (z_o). We take values of these that yield the most conservative values of the observables. The dependences on z_f and z_o are given in the companion technical note.

Some important notes regarding the table:

- If a single range of values is listed for the full set of masses, than the dependence on z_f and z_o is stronger than on mass.

- Neither the scale radius or the virial radius provide a true characteristic extent of the SZ signal, being either too small or too large. The geometrical mean of the two, $r_g = \sqrt{R_v\,r_c}$, is more appropriate.

- The β-profile core radii from theory tend to underpredict the data in massive clusters like CL0016+16; we have artificially extended the upper end of the range by a factor of 2 to accomodate the data.

- In converting from radii to angle, the conversion factor is 2.5 for $z > 1$, increasing to 5 at $z = 0.25$. We have applied 2.5 to the smallest clusters and 5 to the largest clusters to indicate the possible range.

- For tSZ signals, the numbers are underestimates in that the we have taken z_f so as to minimize the signal, but are overestimates for signals at r_c and r_g since these depend on the halo and gas concentrations, which we may have overpredicted. The virial signal values are always underestimates because they do not depend on the concentration parameters.

- For kSZ signals, we have taken the nominal values for a 3.5×10^{14} M$_\odot$ cluster and then fluctuated them up and and down by an *ad hoc* factor of 2.

4

Parameter	Cluster Mass [M$_\odot$]			
	1×10^{14}	3.5×10^{14}	1×10^{15}	3.5×10^{15}
Abundance > M [deg^{-2}]	40	6	0.25	0.012
Number in 20000 deg^2 > M	10^6	10^5	few $\times 10^3$	10^2
virial radius R_v [Mpc]	$1-5$			
β-profile core radius r_c [Mpc]	0.05 - 0.3			
$r_g = \sqrt{R_v\, r_c}$ [Mpc]	$0.2 - 1.2$			
virial angle θ_v [arcmin]	$2.5 - 25$			
core radius θ_c [arcmin]	$0.1 - 0.6$			
$\theta_g = \sqrt{\theta_v\, \theta_c}$ [arcmin]	$0.5 - 4$			
optical depth for Thomson scattering				
central, τ_0	$10^{-3} - 10^{-2}$			
at r_g, τ_g	$10^{-4} - 10^{-3}$			
Comptonization parameter, y				
at r_c	2×10^{-6}	7×10^{-6}	2.5×10^{-5}	1×10^{-4}
at r_g	4×10^{-7}	2×10^{-6}	6×10^{-6}	2.5×10^{-5}
at R_v	$> 7 \times 10^{-8}$	$> 3 \times 10^{-7}$	$> 1 \times 10^{-6}$	$> 4.5 \times 10^{-6}$
tSZ $\Delta T_{\rm CMB}$ at 150 GHz [μK$_{\rm CMB}$]				
at r_c	5	20	65	300
at r_g	1	5	15	70
at R_v	> 0.2	> 1	> 3	> 10
tSZ flux/beam at 150 GHz [μJy]				
at r_c	30	140	450	2000
at r_g	8	35	100	500
at R_v	> 1.4	> 6	> 20	> 90
tSZ total flux at 150 GHz [mJy]	> 0.35	> 3.5	> 24	> 230
	$> 50\ \mu$Jy at 3.5×10^{13} M$_\odot$			
rms peculiar velocity	300 km s^{-1}, $v/c \approx 10^{-3}$			
kSZ $\Delta T_{\rm CMB}$ [μK$_{\rm CMB}$]				
central	$2 - 15$			
at r_g	$0.5 - 4$			
kSZ flux/beam at 150 GHz [μJy]				
central	$30 - 50$			
at r_g	$5 - 15$			
tSZ anisotropy	$\ell \sim 2000 - 20000$			
in $\ell\,(\ell+1)\,C_l/2\pi$	10 μK$^2_{\rm CMB}$			
map rms	7 μK$_{\rm CMB}$			
kSZ anisotropy	$\ell \sim 1000 - 20000$			
in $\ell\,(\ell+1)\,C_l/2\pi$	1 μK$^2_{\rm CMB}$			
map rms	2 μK$_{\rm CMB}$			
Polarized SZ effects	< 10 nK$_{\rm CMB}$			

Table 2: Numerical estimates. See text for notes.

5

4 Detectability of Sunyaev-Zeldovich Signals

Given the above signal levels, what are the necessary integration times and limitations imposed by confusion on detectability of these sources?

4.1 Expected Sensitivity

- **Photometric Sensitivity**: A background-limited 150 GHz photometric camera will in general be limited in sensitivity by telescope loading. Neglecting the $\sqrt{2}$ chopping/sky-subtraction degradation that is being included in sensitivity estimates, such a camera would achieve 2.3 mJy $s^{1/2}$ (310 μK_{CMB} $s^{1/2}$) if we assume 10% telescope emissivity and operation in 1.5 mm PWV conditions. Much can be gained if the telescope emissivity is reduced to 5%: the sensitivity improves by a factor of $\sqrt{2}$ to 1.6 mJy $s^{1/2}$ (220 μK_{CMB} $s^{1/2}$). Assuming $2 f \lambda$ pixels (to ensure dewar loading is small), a 500-pixel focal plane would cover a 20 arcmin × 20 arcmin field-of-view.

  If we include other frequencies under the same conditions, we obtain the sensitivities given in Table 3. The 100 GHz and 150 GHz sensitivities are telescope-limited. The 220 GHz and 275 GHz bands would improve by about $\sqrt{2}$ if either the telescope emissivity were reduced by 2 or if the atmospheric opacity were reduced by 2.

frequency [GHz]	atmosph. transm.	NET_{RJ} [μK_{RJ} $s^{1/2}$]	NET_{CMB} [μK_{CMB} $s^{1/2}$]	NEFD [mJy $s^{1/2}$]
275	0.86	190	1000	2.5
220	0.905	170	530	2.2
150	0.93	180	310	2.3
100	0.93	210	270	2.7

Table 3: Background-limited sensitivities for SZ bands, assuming 10% telescope emissivity and 1.5 mm PWV conditions.

- **Spectroscopic Sensitivity**: A background-limited waveguide spectrometer operating near 150 GHz with 3 GHz resolution should achieve a sensitivity of $\approx 5 \times 10^{-19}$ $W\,m^{-2}$ $s^{1/2}$ for the conservative 10% emissivity assumption. A reduction to 5% emissivity would improve this by about 40%, again a significant gain.

4.2 Naive Integration Times

In Table 4, we list integration times for the various science targets listed in Table 2 using the sensitivities listed in Table 3, neglecting confusion and assuming that the cluster or science target is always on the array. We calculate the time needed to reach $S/N = 5$ in each beam, so that one is truly measuring a profile.

We defer discussion of specific science projects until after confusion has been discussed.

4.3 Confusion Limits

The dominant source of confusion at SZ frequencies is extragalactic infrared point sources. We present confusion limits from A. Blain using the beam parameters given earlier[1]. The *1 source per beam* confusion limits are given in Table 5. The confusion limit at 150 GHz is higher than the tSZ

---

[1]which correspond to poorer angular resolution than one might *a priori* calculate for a 25-m telescope; they are closer to what one might expect from a 20-m telescope. This degradation is due to the conservative edge taper assumed.

target	signal level μK_{CMB}	μJy	time [ksec]	time [hours at 50% obs. eff.]
tSZ profiles, $S/N = 5$ per beam				
at r_g, M $= 3.5 \times 10^{15}$ M$_\odot$	70	500	0.5	0.3
virial wings, M $= 3.5 \times 10^{15}$ M$_\odot$	10	75	24	13
at r_g, M $= 1 \times 10^{15}$ M$_\odot$	15	100	11	6
virial wings, M $= 1 \times 10^{15}$ M$_\odot$	3	23	270	150
at r_g, M $= 3.5 \times 10^{14}$ M$_\odot$	5	35	100	55
virial wings, M $= 3.5 \times 10^{14}$ M$_\odot$	1	7.5	2400	1300
tSZ pt-src survey, $S/N = 5$ at mass limit				
10 deg^2 to 1×10^{14} M$_\odot$	50	350	85	50
0.5 deg^2 to 3.5×10^{13} M$_\odot$	7	50	220	120
tSZ spectroscopy, one beam,				
$S/N = 5$ per $\Delta\nu = 3$ GHz bin				
at r_g, M $= 3.5 \times 10^{15}$ M$_\odot$	70	500	7	4
at r_g, M $= 1 \times 10^{15}$ M$_\odot$	15	100	120	70
kSZ at r_g, $S/N = 5$ per beam	4	30	150	80
assuming typical $v/c = 10^{-3}$	0.5	3.7	9600	5300
tSZ anisotropy, $S/N = 5$ per beam, 1 FoV	7	52	50	30
kSZ anisotropy, $S/N = 5$ per beam, 1 FoV	2	15	600	330

Table 4: Expected integration times to obtain $S/N = 5$ per beam for various science targets, all at 150 GHz.

signal level in the wings of 3.5×10^{14} M$_\odot$ and 1×10^{15} M$_\odot$ clusters and is comparable to the tSZ signal level at r_g in 3.5×10^{14} M$_\odot$ clusters. Confusion is clearly a challenge.

frequency [GHz]	flux density [μJy]	temperature [μK_{CMB}]	y parameter
275	66	27	1.1×10^{-5}
220	89	21	N/A
150	44	6	2.3×10^{-6}
100	21	2.1	5.1×10^{-7}

Table 5: One-source-per-beam confusion limits

It is expected confusion noise may be subtracted using maps made at higher frequencies. The limit on how well this can be done is set by the confusion limit in the higher-frequency bands – assuming one knows the source spectral index perfectly, the systematic error on removing a source based on its high-frequency flux is set by the uncertainty on that high-frequency flux, which can be no smaller than the confusion noise.

Confusion noise is not Gaussian and depends on the source count power-law slope of the confusing source distribution. Nevertheless, it is conventional to require no more than 1 source every 30 beams when considering 5σ point-source detections and no more than 1 source every 10 beams when considering 3σ point-source detections. So, useful figures of merit are obtained by scaling the

350 GHz and 490 GHz 1-source-per-30-beams and 1-source-per-10-beams fluxes to the SZ bands using a standard $\nu^{1.7}$ emissivity law: to first order, we will assume that the 1-source-per-30-beams and 1-source-per-10-beams levels provide the signal levels at which one can obtain no better than $S/N = 5$ and $S/N = 3$ per beam, respectively, in the SZ map.[2] These scaled fluxes are listed in Table 6, which indicate that it is possible to remove sources to well below the 1-source-per-beam confusion limit. Further statistical suppression of confused sources might be obtained by using confused high-frequency maps in some sort of joint multifrequency map estimation.

	350 GHz		490 GHz	
	1 src per	1 src per	1 src per	1 src per
frequency	30 beams	10 beams	30 beams	10 beams
[GHz]	[μJy]	[μJy]	[μJy]	[μJy]
in-band	830	390	1200	500
275	340	160	140	59
220	150	70	62	26
150	36	17	15	6.3
100	8.1	3.8	3.4	1.4

Table 6: Confusion levels in high-frequency bands scaled to SZ bands.

ALMA follow-up to identify and measure the fluxes of confusing point sources in-band is an obvious prospect to consider, but the field-of-view of ALMA is so small that one can only cover small regions to sufficient depth in a reasonable time (see the technical note for integration times, as well as Section 4.4 of this note).

4.4 Candidate SZ Key Projects

Given the above tables of signal levels, integration times, and confusion limits, a number of key SZ science projects suggest themselves, listed in Table 7. We have aimed for a number of programs that each require no more than 100 to 200 hours per year and are conducted over 5-year periods. Based on the observed PWV distributions, it would be reasonable to have about 5 of these projects running at any given time.

In addition to full mapping applications, we have presented two tSZ "radial profile" key projects, in which azimuthal averaging will be used to obtain tSZ radial profiles for large catalogs of sources in reasonable amounts of telescope time. Of course, detailed information about azimuthal variations is lost. Expected profiles with uncertainties are shown in Figure 2. The choice of sensitivities for these projects was made so as to achieve $S/N \approx 5$ in each radial bin at large radius. This sensitivity easily allows one to distinguish the three different β-profile exponents $\beta = 0.6$, 0.67, and 0.75. The per-beam sensitivity needed to obtain these radial profiles is a factor of 10 poorer than what is needed for full mapping, enabling the study of 100 times as many clusters.

Quantitative evaluation of the scientific merit of these projects awaits detailed simulation work, which will be undertaken during the ongoing CCAT study. But one can reach some basic conclusions about the relative merit and feasibility of the various key projects:

- The most obviously worthwhile programs are the pure tSZ mapping and radial profile studies

---

[2]It only takes 1200 sec and 4500 sec to reach the confusion limits on one field-of-view at 350 GHz and 490 GHz, respectively, according to numbers from A. Blain and T. Herter. Covering an entire 20 arcmin × 20 arcmin SZ field is only challenging if the high-frequency camera field-of-view is as small as 5 arcmin × 5 arcmin, and, even then, should only take 72 ksec at 490 GHz.

Science target	per beam sensitivity μK_{CMB}	μJy	S/N	# of objects per year	# of hours per year	# of objects in 5 years	# of hours in 5 years	confusion (# srces per 490 GHz beam)
tSZ profiles								
High-mass ($> 3.5 \times 10^{15}$ M$_\odot$)								
mapping	2	15	5	10	130	50	650	1 per 30
Medium-mass (1×10^{15} M$_\odot$ $- 3.5 \times 10^{15}$ M$_\odot$)								
mapping	1	7.5	3	3	160	15	800	~ 1 per 10
radial profile	10	75	0.3	200	100	1000	600	$\ll 1$ per 30
Low-mass (3.5×10^{14} M$_\odot$ $- 1 \times 10^{15}$ M$_\odot$)								
radial profile	3	23	0.3	20	120	100	600	< 1 per 30
tSZ pt-src survey, $S/N = 5$ at 1×10^{14} M$_\odot$ on 10 deg^2 fields								
	10	75	5	1	50	5	150	$\ll 1$ per 30
tSZ spectroscopy								
High-mass ($> 3.5 \times 10^{15}$ M$_\odot$)								
9 points $\theta < \theta_g$	14	100	5	4	140	20	700	< 1 per 30
Medium-mass (1×10^{15} M$_\odot$ $- 3.5 \times 10^{15}$ M$_\odot$)								
1 point $\theta < \theta_g$	3	20	5	2	140	10	700	~ 1 per 30
kSZ detection at $S/N = 1$ per 150 GHz beam (for 4 μK_{CMB} signal level)								
150 GHz	4	30	1	5	17	25	80	< 1 per 30
220 GHz	5.9	25	0.7	5	20	25	110	1 per 10
275 GHz	7.3	18	0.55	5	50	25	260	~ 1 per 1?
tSZ anisotropy survey, $S/N = 5$ per beam, 0.5 deg^2 fields								
	1.4	10	5	1	120	5	600	1 per 10–30
kSZ anisotropy survey, $S/N = 1$ per 150 GHz beam, FoV-size fields								
150 GHz	2	15	1	1	13	1	65	1 per 30
220 GHz	2.9	12	0.7	1	19	5	95	~ 1 per 1?
275 GHz	3.7	9	0.55	1	40	5	200	~ 1 per 1?

Table 7: Candidate SZ key projects. The "confusion" column refers to the number of sources per 490 GHz beam at the flux level obtained by scaling the low-frequency per-beam sensitivity to 490 GHz using $\nu^{3.7}$.

given that the number of objects obtained is large and confusion is not much of a problem.

- Blind tSZ surveying down to 1×10^{14} M$_\odot$ ($S/N = 5$) over many square degrees is feasible and not limited by confusion noise.

- tSZ spectroscopy is fast enough that an interestingly large sample of objects can be observed. It seems appropriate to view spectroscopy as a follow-on project to the tSZ profiles, especially because it requires a special-purpose low-R spectrometer.

- The kSZ studies are stymied by confusion noise. The raw sensitivity is more than sufficient, but confusion promises to be limiting at 220 GHz and 275 GHz with CCAT alone, even after designing the surveys to be quite shallow ($S/N = 1$ per 150 GHz beam) and using higher-frequency bands to detect and remove confusing sources. Even using ALMA, it is not possible
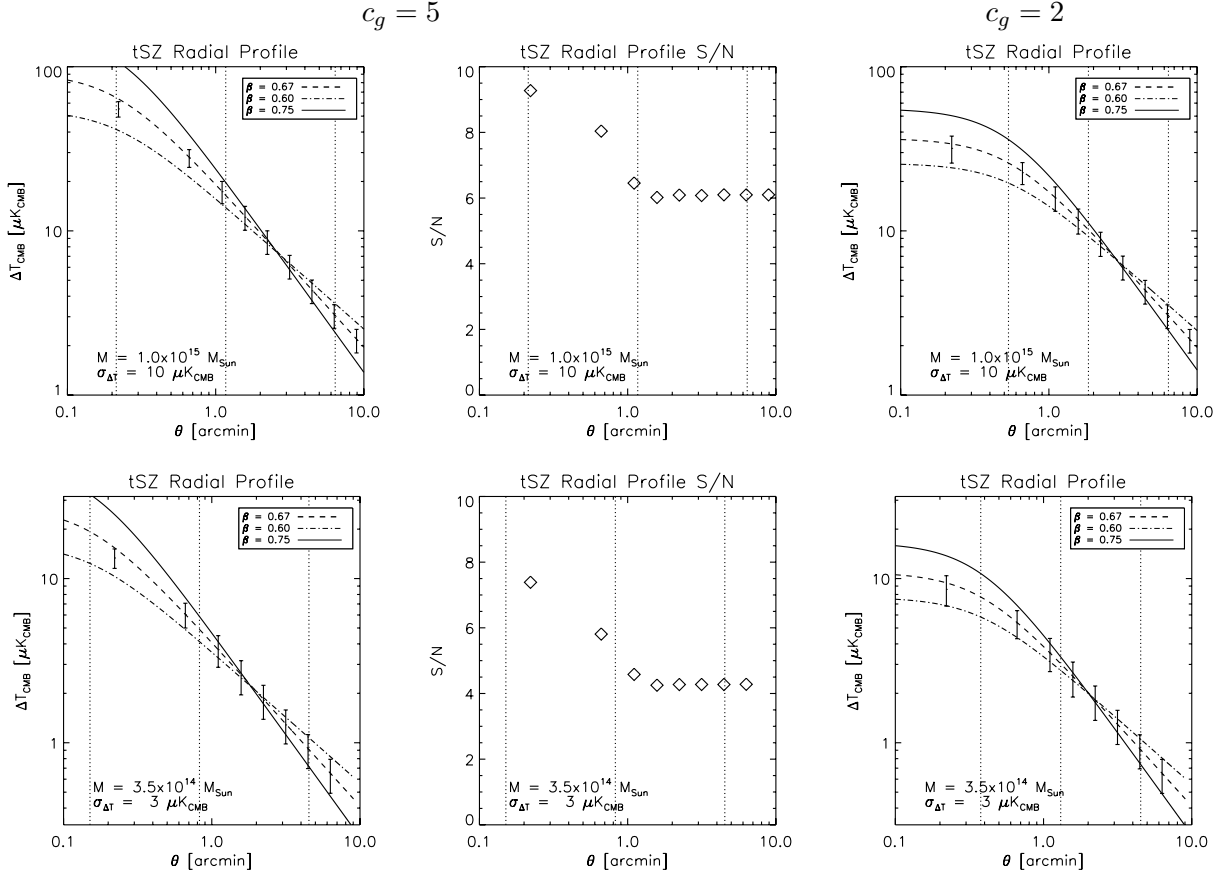
Figure 2: Expected errors on tSZ radial profiles. Cluster masses and assumed per-beam sensitivies are indicated. Each plot also shows three different β profiles that would yield the same integrated SZ Comptonization parameter within R_v. Profiles for two different values of the gas concentration factor, c_g, are shown; c_g is the ratio of the dark-matter halo NFW scale radius to the the gas β-profile core radius. The vertical dotted lines indicate the three radii r_c, r_g, and R_v. The radial binning of the data is linear at small radius and logarithmic at large radius; no bin is allowed to be smaller than the beam FWHM at 150 GHz. The increase with radius of the area per bin yields approximate constant $S/N \approx 5$ at large radius.

> to subtract sources to a sufficiently small flux over a large enough area to make kSZ detection likely.[34]

- For similar reasons, attempts to confirm tSZ signals using 220 GHz and 275 GHz are difficult except for the most massive clusters.

One should not take the last two conclusions as the final word for a number of reasons:

1. They certainly should be reevaluated if significant revisions in the infrared galaxy number

---

[3]Observing down to 10 μJy at 275 GHz over 10 arcmin^2 – the size of the core of a cluster out to θ_g – would require about 1 Msec. The 100 arcmin^2 needed to observe kSZ anisotropy would take 10 Msec. Even covering 1 arcmin^2 would require 100 ksec.

[4]For an explanation of why CCAT seems to suffer worse confusion limitations than APEX, ACT, or SPT, see the companion technical note.

counts are made; the models predicting these counts are not yet precisely constrained – part of the reason to build CCAT!

2. More detailed and accurate predictions of tSZ and kSZ signal levels may result in larger values; we have expressly tried to be conservative.

3. Simulations of maps at the three frequencies may indicate that confusion is more removable than we have claimed here.

4. Gravitational lensing by the clusters under study has not been taken into account; lensing will mitigate confusion to some extent.

Nevertheless, given the large uncertainty in the ability to do SZ work at 220 GHz and 275 GHz, and the obvious additional instrumental complication, it seems safe to conclude that the initial focus should be on 150 GHz tSZ observations.

5   Telescope Requirements

The requirements on the telescope imposed by the above science goals are summarized in Table 8.

Item	Requirement	Goal	Notes
Aperture	≥ 20 m	–	uniqueness
Surface roughness	$< 30 \ \mu$m	–	$\lambda/20$ at 490 GHz
Blockage/loading	$< 10\%$	$< 5\%$	goal: telescope loading no worse than atmosph. and dewar loading
Wavelength range	2 mm	$1 - 2$ mm	SZ obs
	620, 850 μm	same	IR pt src removal
Field-of-view diameter	10 arcmin	20 arcmin	contain entire cluster
Pointing			
on-the-fly	25 arcsec	12 arcsec	1 beam at 1–2 mm
reconstructed	1.25 arcsec	0.6 arcsec	beam/20 at 1–2 mm
on-the-fly	6 arcsec	same	1 beam at 620 μm
reconstructed	0.3 arcsec	same	beam/20 at 620 μm
Tracking			
one hour	1.5 arcsec	same	do 1 hour obs w/o
20 min	same	same	added pointing
10 sec	same	same	jitter
Elevation Limits	> 30	–	Planck sources
Scan speed	0.5 deg/sec	1 deg/sec	sky noise
	on FoV-sized fields (Lissajous)		
Spectroscopy		$\Delta\nu = 3$ GHz	2 bands, $120 - 180$ GHz
		$120 - 325$ GHz	and $200 - 325$ GHz
Polarization capability	–	–	

Table 8: Telescope requirements arising from science goals.

6 Uniqueness and Complementarity

SZ instrumentation on CCAT would probe a unique combination of angular scales and frequencies and would complement other SZ projects:

- The large-area blind tSZ surveys by APEX-SZ, ACT, and SPT are optimized for detection of clusters down to 3.5×10^{14} $M_\odot$, but have angular resolution too poor to study the SZ spatial profile in any detail for the bulk of the clusters they will detect. Planck's angular resolution is even poorer, ~ 4 arcmin at 150 GHz, and hence its mass limit is even higher, $\sim 8 \times 10^{14}$ $M_\odot$. CCAT follow-up on a subsample of clusters detected in these surveys will provide spatially resolved SZ profiles and possibly SZ-based gas temperatures. By no means will CCAT cover an exhaustive sample – only ten to tens of clusters in the various mass ranges – but it will provide detailed information on a much larger sample than any other instrument at millimeter wavelengths. Such data would enable characterization of the mapping from SZ flux to cluster mass, which is expected to depart from simple expectations due to imperfect isothermality. SZ data may in fact be critical for such work, as Chandra and XMM-Newton will not be available to provide X-ray data after the end of the decade and Constellation-X's launch date is now no earlier than 2016. Even with these satellites available, the lowest mass clusters at the highest redshifts might not be accessible due to cosmological dimming.

- A CCAT blind tSZ survey would have a lower mass limit than those performed with APEX-SZ, ACT, SPT, and Planck. CCAT observations could thus be used to cross-check the large-area surveys' detection efficiency functions.

- The Sunyaev-Zeldovich Array (SZA) is an interferometer designed for blind tSZ surveying at 30 GHz. It is sited at CARMA and is currently taking survey data. It will begin to study cluster substructure at 90 GHz. The SZA, being an interferometer, will have a better understanding of systematic effects of observing technique but will have significantly poorer instantaneous sensitivity due to its factor of 6-7 smaller collecting area, poorer site, and use of heterodyne receivers. Together, SZA and CCAT will provide SZ spectral coverage at high angular resolution from 30 GHz to 150 GHz (and possibly 275 GHz).

  A possible eventual upgrade of SZA for higher frequency operation is not likely to pose much competition to CCAT given the latter's better site and more sensitive receivers.

- The Penn Array is a 64-pixel 90 GHz bolometric array being built for the Green Bank Telescope (GBT). The instrument will have angular resolution 8 arcsec (0.13 arcmin) and 0.5 arcmin field-of-view, which enables it to investigate SZ substructure on few arcsec scales, but it will lose sensitivity on arcminute scales due to sky noise; it thus complements CCAT.

- The Large Millimeter Telescope (LMT) will provide information on scales comparable to GBT or midway between CCAT and GBT. The LMT design provides a 4 arcmin field-of-view, and currently planned instrumentation (AzTEC) will cover a 1.5 arcmin field-of-view. The LMT angular resolution at 150 GHz is comparable to that of GBT at 90 GHz. Atmospheric conditions might favor 90 GHz operation instead, in which case LMT provides angular resolution midway between that of CCAT and GBT. The better angular resolution of the LMT in the 150-300 GHz range as compared to CCAT is cancelled by CCAT's ability to observe in the 350 GHz and 490 GHz bands, which are inaccessible to LMT.

- Interferometers like CARMA and ALMA will have exquisite sensitivity over a field-of-view of a fraction of an arcmin^2 at the frequencies of interest for SZ. They will provide high angular

resolution probes of substructure in the SZ, but will have poor fidelity on scales much larger than 1 arcmin, as well as being too slow to map fields appreciably larger than 10 arcmin^2.

Lastly, it is useful to note that SZ instrumentation makes the least stringent demands on telescope performance and weather, except for requirements on telescope optical loading. Therefore, SZ instrumentation may be most effective in delivering cutting edge science from the earliest commissioning phase and during the poorest weather periods of the year.